Journal of Magnetic Resonance 192 (2008) 329–337

Contents lists available at ScienceDirect

Journal of Magnetic Resonance

journal homepage: www.elsevier.com/locate/jmr

Towards beyond-1 GHz solution NMR: Internal ^{2}H lock operation in an external current mode

Yoshinori Yanagisawa [a,b], Hideki Nakagome [b], Masami Hosono [c], Mamoru Hamada [d], Tsukasa Kiyoshi [e], Fumio Hobo [a,f], Masato Takahashi [a], Toshio Yamazaki [a], Hideaki Maeda [a,f,*]

[a] Genomic Sciences Center, RIKEN, 1-7-29, Suehiro-cho, Tsurumi-ku, Yokohama, Kanagawa 230-0045, Japan
[b] Faculty of Engineering, Chiba University, Chiba 236-8522, Japan
[c] JEOL Ltd., Akishima, Tokyo 196-8558, Japan
[d] Kobe Steel, Ltd., Kobe, Hyogo 651-2271, Japan
[e] Superconducting Materials Center, National Institute for Materials Science, Tsukuba, Ibaraki 305-0003, Japan
[f] Graduate School of Yokohama City University, Yokohama, Kanagawa 230-0045, Japan

ARTICLE INFO

Article history:
Received 30 January 2008
Revised 7 March 2008
Available online 29 March 2008

Keywords:
Ultra high magnetic field
High temperature superconductor
External DC power supply
Field fluctuation
External current mode
Internal deuterium lock
Persistent current mode
NOESY
HSQC
Ubiquitin

ABSTRACT

We have commenced a project to develop a beyond-1 GHz solution NMR spectrometer using a HTS coil. Due to a small residual resistance present in the HTS conductor and joint resistance between conductors, a stable persistent current sufficient for NMR measurements is unlikely. Therefore, a current has to be supplied to the HTS coil from an external power supply. The ripple of an external power supply causes a field fluctuation which must be stabilized. In this study we show results of NMR measurements using a 500–600 MHz NMR in such an external current mode: the field fluctuations are stabilized by an internal ^{2}H lock. The field fluctuation from the external power supply comprises a major field fluctuation component at low frequencies, 0.003–0.005 Hz, and superimposed minor field ripples at 2 Hz and 50 Hz. The former limits the time interval of the internal ^{2}H lock, while the latter generates sidebands in the NMR spectrum. Sideband and baseline noise are controlled by appropriate selection of the feedback loop parameters of the lock. The quality of the 1D-solution NMR spectra observed in external current mode is equivalent to that obtained in persistent current mode. However, if the feedback loop time is as short as the gradient pulse width, refocusing of the NMR signal is lost and NMR peaks disappear. The 2D-NOESY and the 2D-HSQC spectra of ubiquitin in an external current mode have been acquired. The quality of the 2D spectra is equivalent to those obtained in persistent current mode; i.e. the internal ^{2}H lock operates stably over an experimental time interval of 40–50 min. To realize a beyond-1 GHz NMR spectrometer, further investigations must be made of (i) the long term stability of a DC power supply, (ii) the enhancement of the compensation field limit for the internal ^{2}H lock, (iii) the extension of the helium refill time interval, and (iv) a method to correct the field homogeneity in the external current mode.

1. Introduction

Nuclear Magnetic Resonance (NMR) is widely used in biology, materials science, chemistry and physics [1]. As the sensitivity, i.e. the signal-to-noise ratio, and resolution of the technique improve with increments in the magnetic field strength, researchers pursue ever higher field strengths [2]. In the case of protein structure determination by solution NMR, transverse relaxation-optimized spectroscopy (TROSY) [3] and cross relaxation-enhanced polarization transfer (CRINEPT) [4] have enhanced NMR sensitivity to large proteins at a field around 1 GHz. In the field of materials science, the solid-state NMR sensitivity to quadrupole nuclei, such as ^{27}Al [5] and ^{17}O [6], is proportional to the 2.5 power of the magnetic field; thus, a higher field is desirable. To this point, a field of 950 MHz (22.3 T) has been achieved [7] through the use of low temperature superconductors (LTS). Although the critical current density at high fields is increased by increasing the tin content of a bronze matrix [8] or by the adoption of the restacked rod fabrication process (RRP) for the Nb_3Sn conductor [9], 1 GHz is still the upper limit on available NMR fields.

Using a high temperature superconductor (HTS) such as a Bi2223 tape conductor [10] for the high field part of an NMR magnet might permit the accessible fields to exceed 1 GHz, as long as the upper critical field of the HTS is sufficiently high. We have commenced a project to develop a beyond-1 GHz NMR [11] using a HTS; the LTS innermost coil of the 920 MHz NMR magnet installed in the National Institute for Materials Science (NIMS) [2] is to be

* Corresponding author. Address: Genomic Sciences Center, RIKEN, 1-7-29, Suehiro-cho, Tsurumi-ku, Yokohama, Kanagawa 230-0045, Japan. Fax: +81 045 508 7360.
E-mail address: maeda@jota.gsc.riken.jp (H. Maeda).

1090-7807/$ - see front matter © 2008 Elsevier Inc. All rights reserved.
doi:10.1016/j.jmr.2008.03.015

replaced by a Bi2223 HTS coil. Due to a residual resistance present in the HTS tape conductor [12] and to joint resistance between HTS conductors, attaining a stable persistent current sufficient for NMR measurement is unlikely. Therefore, an external power supply must provide current for the HTS coil [13]. However, the ripple current from this power supply causes a field ripple which, for solution NMR, requires stabilization to a level less than 0.1 ppb (10^{-10}); we represent the field ripple by the normalized value $\Delta B/B_0$, where B_0 is the central field of the NMR magnet and ΔB is a field fluctuation.

Ultra-high fields over 40 T are achievable with the use of a water-cooled resistive magnet or a hybrid magnet [14]; the latter comprises a superconducting backup coil and a water-cooled resistive inner coil [5,14]. The coil current for the resistive coil is supplied by a 10-MW class power supply. The ripple field amplitude ranges between 10 ppm and 100 ppm [15]. Its causes include instability in the power supply current, a winding motion generated by electromagnetic forces and water flow, and variations in water temperature [16]. Due to the AC line voltage [15], the field fluctuation spectrum has peaks at 50 Hz and its harmonic frequencies. Sigmund et al. [17] have suggested mounting an inductive shielding inside the probe, which reduces the 60 Hz frequency component. Iijima et al. [18] have demonstrated that deconvolution of the free-induction decay (FID) signal using the field fluctuation signal results in a reduction in modulation. Though these methods are useful for a resistive NMR magnet, they are not necessarily useful for solution NMR in an external current mode, as the latter requires a sufficient removal of the low-frequency field fluctuation.

In the case of a LTS NMR magnet, an injection of the magnetic flux by the secondary winding compensates for the fast decay of the persistent field [19,20]. Though this method effectively counteracts the persistent field decay, the flux injection induces an additional field fluctuation; therefore, it is not suitable for solution NMR.

Bascunan et al. [21] have achieved a ^{1}H NMR spectrum with a 700 MHz NMR magnet operated in external current mode; the magnet comprises an LTS low field coil and an HTS high field coil. Though they obtained the first continuous wave solution NMR spectrum in the external current mode, they neither used a field-frequency lock nor room temperature shims, and the spectrum's half height line width was as large as ~kHz. Evidently, to obtain better sensitivity and better resolution, investigators must use FT NMR and a phase sensitive field-frequency lock.

A straightforward way to stabilize the field fluctuation for solution NMR is to use an internal-^{2}H lock [1]. The lock has been, however, developed to stabilize a persistent current drift ~10 ppb/h. It is not clear whether the internal ^{2}H lock is applicable to the NMR spectrometer operated in an external current mode. Even with the best available DC power supply, the field fluctuation is as large as ~1 ppm in amplitude, and comprises various frequency components in the range of 0.001 Hz [22] to 50 Hz. To investigate the applicability of the internal ^{2}H lock to a solution NMR spectrometer operated in an external current mode, it is necessary to evaluate (a) the field fluctuation spectra from a power supply and (b) the limit of the field compensation by the internal ^{2}H lock. If the latter is larger than the former, the internal ^{2}H lock compensates for the field fluctuation and vice versa. Such a correlation, so far unexplored, is investigated here.

The ultra high-field NMR spectrometer is especially useful for protein structure determination through a multi-dimensional NOESY experiment [23]. A slight-instability in the lock operation during a NOESY measurement results in noticeable T_1 noise and water signal. To this point, external current mode, multi-dimensional NMR spectra such as NOESY and HSQC have never been achieved; they are demonstrated in this paper.

In summary, the topics investigated here are as follows: (a) an NMR magnetic field fluctuation spectrum taken in external current mode, (b) the frequency response characteristics and maximum permissible field fluctuation amplitude for the internal ^{2}H lock, and (c) the quality of 1D- and 2D-solution NMR spectra in external current mode either for standard test samples or a protein solution. Finally, we will discuss the effect of these results on the future of beyond-1 GHz NMR spectroscopy, and present suggestions for overcoming the associated problems.

2. Experimental procedure

2.1. Magnetic field fluctuation

A 500 MHz NMR magnet, made by Bruker Biospin, was charged by a highly stabilized external DC power supply [22] to provide the operating current. The superconducting switch connected in parallel to the NMR coil had been "open" (in the resistive state) before the current rise. The current stability of the DC power supply was <10 ppm in peak–peak amplitude over an hour; this level is about an order of magnitude smaller than a conventional DC power supply. A 600 MHz NMR magnet [19] made by JASTEC was also used for the experiment.

While the operating current was supplied by the external DC power supply, the coil voltage, $v(t)$, was measured by a digital data recorder every 2 ms. The $v(t)$ was then Fourier transformed and divided by a coil impedance $j\omega L$, resulting in a coil current $I(\omega)$ in the frequency domain; here ω is the angular frequency and L is the coil inductance. An inverse Fourier transform of $I(\omega)$ gives the ripple current $i(t)$ in the time domain; these are equivalent to the field fluctuation.

2.2. Frequency response and maximum permissible fluctuation for the internal ^{2}H lock

A solution NMR spectrometer usually contains an internal ^{2}H lock [1]. It measures the ^{2}H NMR signal in the phase sensitive mode; the dispersion signal is used for field stabilization, and the absorption signal for field homogeneity. The dispersion signal at the lock frequency provides an error signal for the feedback loop of the lock system; it corresponds to the deviation from the lock frequency [1]. The error signal goes to the PI controller, giving a control signal to the power source of a field compensation coil. The performance of the feedback loop is determined by loop parameters, such as loop gain, loop time and loop filter.

The effect of external field fluctuations on the internal ^{2}H lock was investigated by the model experiment illustrated in Fig. 1. A modulation solenoid, 32 mm in diameter and 68 mm in height, was installed inside a ^{1}H selective probe for a 500 MHz NMR spectrometer, DMX 500 made by Bruker Biospin. The solenoid generates a sinusoidal field; it is 0.001–2 ppm in amplitude and 0.01–300 Hz in frequency.

If a sufficiently high sinusoidal field is applied, the internal ^{2}H lock cannot compensate for the external field ripples. In that case, as shown in Fig. 1, a sinusoidal wave appears on both the error signal and the controller output signal. However, if the external sinusoidal field is fully stabilized by the internal ^{2}H lock, the error signal is zero. We evaluated both the error signal amplitude and the controller output signal amplitude as a function of the sinusoidal field frequency and amplitude. Simultaneously, we measured the NMR spectra for 1% $CHCl_3$ in acetone-d_6.

2.3. 1D and 2D NMR measurement in external current mode

At first, the 500 MHz NMR magnet was operated in the persistent current mode; the field homogeneity was corrected both by

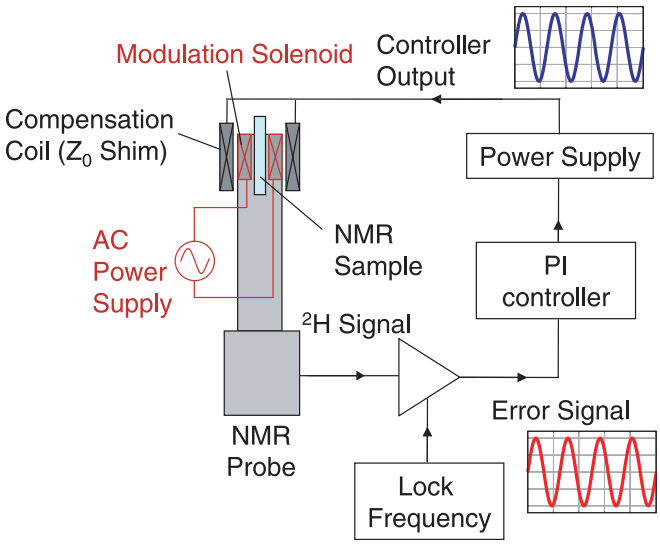

Fig. 1. A schematic drawing of a model experiment; a modulation solenoid is installed inside a ^{1}H probe, connected to an AC power source. If a sample field oscillates in locked mode, the sinusoidal wave appears on the error signal and the controller output signal. NMR spectra are measured in the presence of the sinusoidal field generated by the modulation solenoid.

a gradient shimming and by room temperature shims. The magnet was then connected to the external DC power supply, and the current was raised to the operating value, with the superconducting switch being "closed" (in the superconducting state). Finally, the superconducting switch was set to "open" (the normal state), resulting in operation in the external current mode. The NMR spectra were measured by a TXI probe.

The magnetic field changes after a persistent current switch opens. Thus, the NMR measurement was carried out after the initial field change ceased. The quality of the 1D NMR spectra and 2D NMR spectra were assessed by the following experiments:

(a) A long term stability test of the NMR spectra for 1% $CHCl_3$ in acetone-d_6, including a comparison of the NMR spectra with and without the internal ^{2}H lock.
(b) A ^{1}H line shape test for 1% $CHCl_3$ in acetone-d_6, including an investigation of the effect of the loop parameters on the NMR spectra.
(c) A ^{1}H sensitivity test for 0.1% ethylbenzene in $CDCl_3$.
(d) A water suppression test for 2 mM sucrose with 0.5 mM DSS, and 2 mM NaN_3 in 90% H_2O and 10% D_2O, the water suppression being achieved either by presaturation or by the use of 3919WATERGATE.
(e) 2D NMR tests such as NOESY and ^{15}N-HSQC for a double-labeled 2 mM chlorella ubiquitin, with 50 mM K-Phosphate and 1 mM NaN_3 in 90% H_2O and 10% D_2O. Here, water suppression was achieved either by presaturation or by the use of 3919WATERGATE. The mixing time for the NOESY was 0.1 s and the repetition time was 1 s. The number of signal points along the T_2 axis was 1024, while that along the T_1 axis was 256. The time to acquire the experimental data was about 40 min.

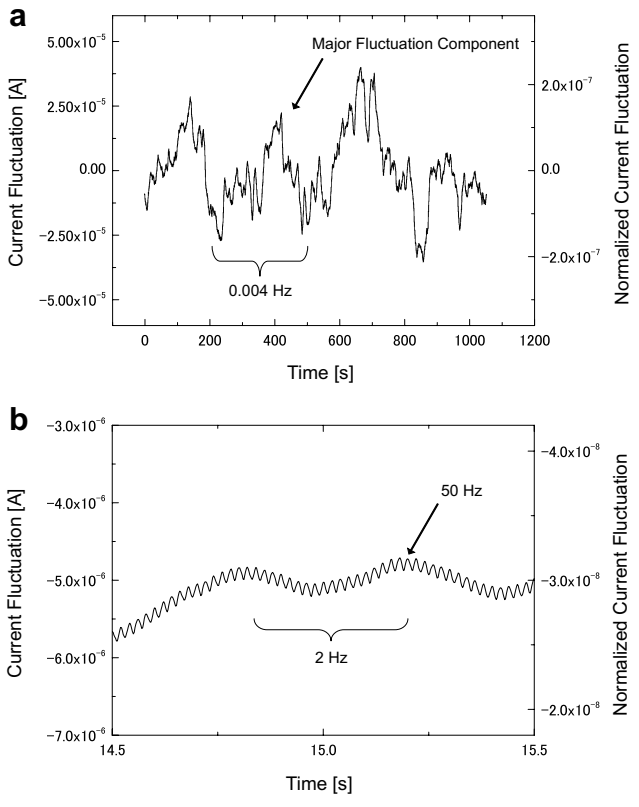

Fig. 2. (a) Current fluctuation, $i(t)$, over 1050 s. The current fluctuation is indicated on the left axis, while the normalized current fluctuation (=current fluctuation/operating current) is shown on the right axis. (b) The changes in $i(t)$ over 1 s. The field fluctuation comprises a major fluctuation component at 0.003–0.005 Hz and minor ripple field at 2 Hz and 50 Hz. The results are obtained for the 600 MHz NMR magnet in the external current mode.

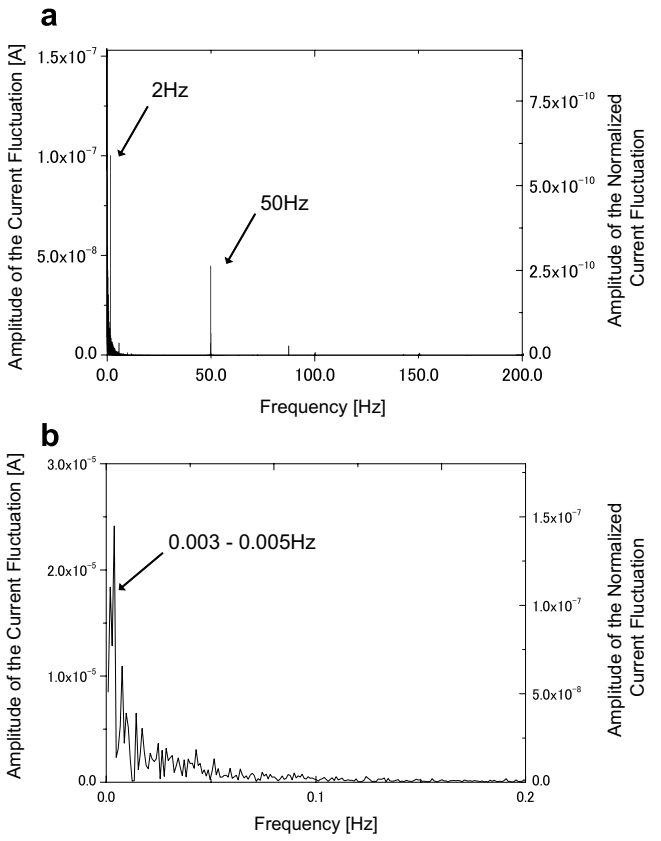

Fig. 3. (a) The current fluctuation spectrum, $I(\omega)$, in the range from 0 Hz to 200 Hz and (b) $I(\omega)$ in the range from 0 Hz to 0.2 Hz. The current fluctuation spectra is indicated on the left axis, while the normalized current fluctuation spectra (=$I(\omega)$/operating current) is on the right. The spectra are obtained for the 600 MHz NMR magnet.

3. Experimental results and discussion

3.1. Field fluctuation spectra

Fig. 2(a) and (b) represents the changes in time of the ripple current, $i(t)$, over 1050 s. The data obtained is based on the coil voltage for the 600 MHz NMR magnet operated in the external current mode. The fluctuation current value is indicated on the left axis, while the normalized current fluctuation (=the current fluctuation/the operating current) is shown on the right axis. The current rises and falls irregularly, with a peak–peak amplitude of 4.5×10^{-7} (0.45 ppm). It comprises a major fluctuation component at low frequencies of 0.003–0.005 Hz (see Fig. 2(a)) and superimposed minor ripples of ~2 Hz and 50 Hz (see Fig. 2(b)).

The normalized current fluctuation spectra in external current mode are shown in Fig. 3(a) and (b). Large peaks are present below 0.05 Hz, which correspond to the main fluctuation component seen in Fig. 2(a); they may be due to the temperature fluctuation of the current transducer and the current controller of the DC power supply. The 2 Hz peak seen in Fig. 3(a) may be related to the feedback loop time of the controller in the power supply; the 50 Hz peak is caused by the rectified AC line voltage.

3.2. Frequency response and permissible external field fluctuation for the internal ^2H lock

Fig. 4 compares an NMR spectrum with and without the internal ^2H lock, in the presence of an external sinusoidal field. The NMR sample used was 1% $CHCl_3$ in acetone-d_6. The sinusoidal field generated by the modulation solenoid is 0.05 ppm in amplitude and the feedback loop time is 0.083 s. The field compensation is better at low frequencies. In the case of the 0.1 Hz ripples, the internal ^2H lock fully compensates for the external ripple field, as shown by the absence of sidebands in the locked spectrum in Fig. 4(b). In contrast, for the 2 Hz ripples, the external ripple field is only partially damped; consequently, sidebands are observed (see Fig. 4(b)), though they are much smaller than those for the unlocked spectrum seen in Fig. 4(a). At 50 Hz, the external ripple field is not at all neutralized, and the sidebands with and without the deuterium lock are nearly the same.

If we assume a FID from a sample with only one peak, f_0, and it is modulated by an external sinusoidal field, that FID is represented as [24]

$$V_0 \exp\left(-\frac{t}{T_2}\right) \sin\left(2\pi f_0 t - \frac{\Delta f}{f_m}\cos(2\pi f_m t + \phi)\right), \quad (1)$$

where V_0 is the initial FID amplitude, t is the time, T_2 is the transverse relaxation time, Δf is the ripple amplitude, f_m is the ripple frequency and ϕ is the ripple phase. A Fourier transformation of Eq. (1) gives a NMR spectrum. The experimental spectrum for f_m = 2 Hz and Δf = 25 Hz (0.05 ppm) seen in Fig. 4(a) coincides with the simulated spectrum for f_m = 2 Hz and Δf = 2.5 Hz (0.005 ppm); i.e. the 2 Hz ripple field is reduced 10-fold by the internal ^2H lock. The ratio remains unchanged until the external sinusoidal amplitude, Δf, exceeds 250 Hz (0.5 ppm).

When the sinusoidal field is applied, the controller output signal shows a sinusoidal wave, as in Fig. 1. Fig. 5(a) shows the frequency response of the controller output amplitude gain, corresponding to the relative ratio of the compensation field to its sinusoidal field, for loop times of 0.003 s, 0.083 s and 0.384 s. It is flat and assumed to be 0 dB (=1) at lower frequencies, and then it reaches a maximum at the resonance frequency. The lines included in Fig. 5(a) represent theoretical values based on the second-order lag element model [25]. The phase shift in Fig. 5(b) is calculated by this model, on the basis of the amplitude gain depicted in Fig. 5(a).

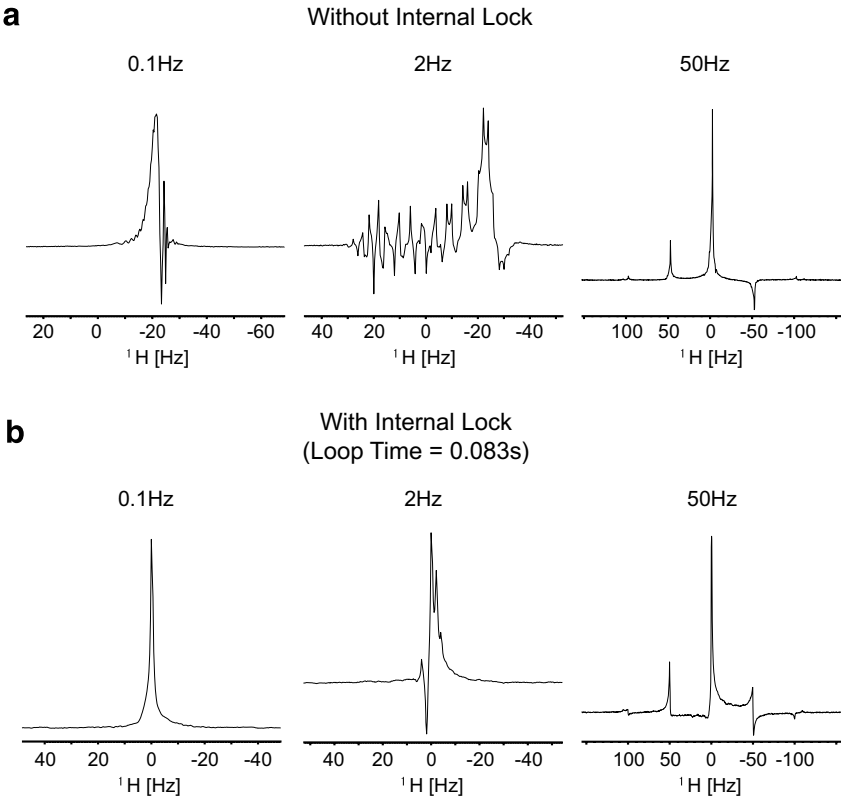

Fig. 4. NMR spectra with/without the internal ^2H lock for various sinusoidal field frequencies; the sample is 1% $CHCl_3$ in acetone-d_6; the sinusoidal field amplitude is 0.05 ppm and the feedback loop time is 0.083 s. (a) Unlocked mode NMR spectra in the presence of 0.1 Hz, 2 Hz and 50 Hz sinusoidal fields, respectively. (b) Locked mode NMR spectra in the presence of 0.1 Hz, 2 Hz and 50 Hz sinusoidal fields, respectively.

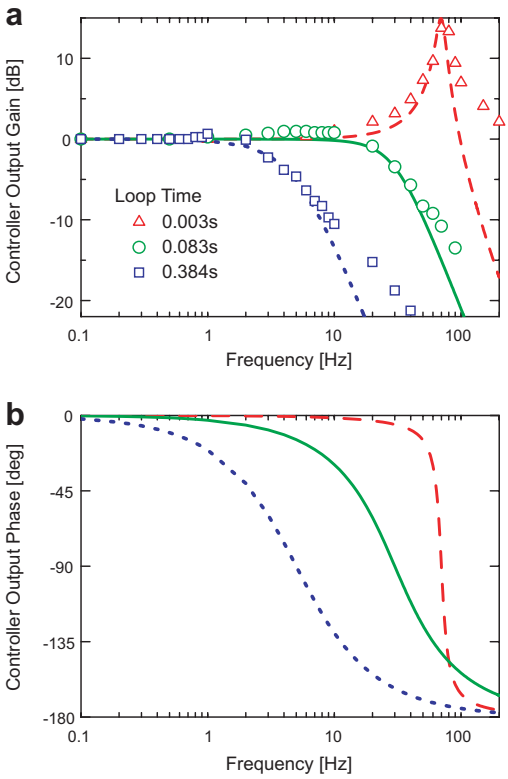

Fig. 5. (a) Frequency response of the controller output signal gain. The sinusoidal field amplitude Δf is 0.05 ppm. Open triangles indicate the experimental result for a 0.003 s loop time, open circles that for 0.083 s, and open squares that for a 0.384 s loop time. The broken line indicates the calculated curve based on a second-order lag element model for the 0.003 s loop time; the solid line is that for 0.083 s, and the dotted line is that for 0.384 s. (b) Frequency response of the calculated phase shift for the controller output signal based on the second-order lag element model. The dashed line indicates the calculated curve for a 0.003 s loop time, the solid line that for 0.083 s, and the dotted line that for 0.384 s.

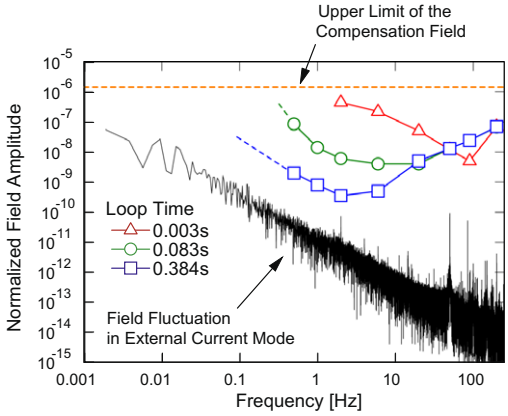

Fig. 6. Comparison between the field fluctuation amplitude spectra in external current mode and the external sinusoidal field amplitude giving a modulated-sideband height of 5% of the main peak; open triangles, open circles, and open squares are the results for loop times of 0.003 s, 0.083 s, and 0.384 s, respectively. The vertical scale is normalized to the operating field. The horizontal broken line at 1.5×10^{-6} (1.5 ppm) is the upper limit on the compensation field provided by the lock.

For the loop time of 0.083 s, indicated by the open circles and solid line in Fig. 5, the gain at 0.1 Hz is 0 dB and the phase shift is zero; therefore, the external field is fully compensated for by the lock. At 2 Hz, the gain is 0.1 dB and the phase shift is −5 deg, values indicating the partial compensation seen in Fig. 4(b). At

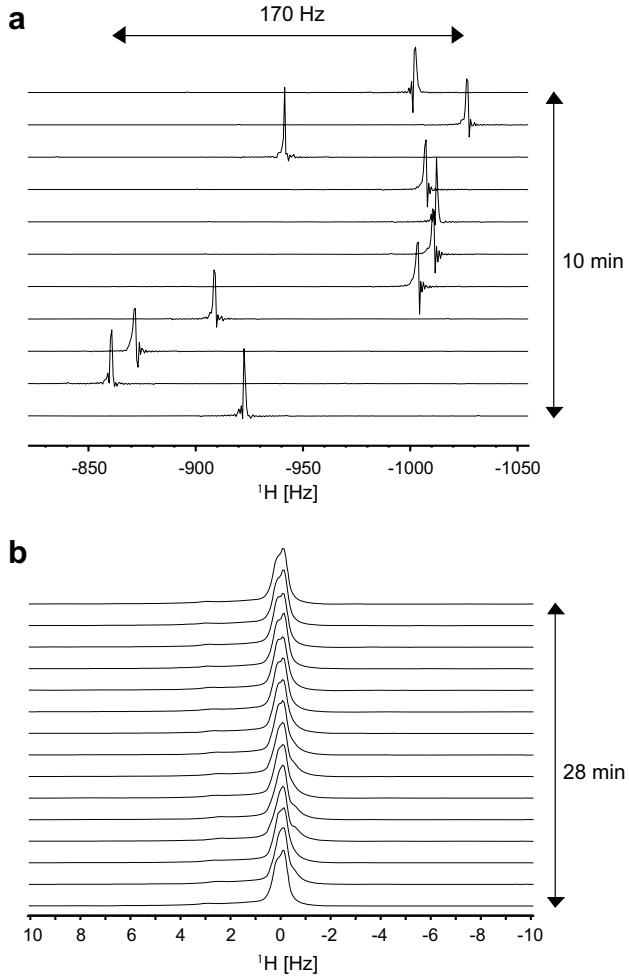

Fig. 7. (a) NMR peaks without an internal ^{2}H lock over 10 min; the spectrometer is operated in external current mode. The sample is 1% $CHCl_3$ in acetone-d_6. The NMR peak fluctuates irregularly with a peak–peak amplitude of 170 Hz (0.34 ppm). (b) Effect of an internal ^{2}H lock on the peak frequency and line shape in external current mode; both the peak frequency and the line shape are constant. The data were taken over a period of 28 min.

50 Hz, the gain is −8.4 dB and the phase shift is −124 deg; therefore, the external field is nearly uncompensated. For the loop time of 0.003 s, indicated by the open triangles and the broken line in Fig. 5, the frequency response is better. However the gain attains a maximum of 15 dB (=5) at 70 Hz. Thus, an overcompensation might be expected; the lock adds an extra sinusoidal field, increasing the baseline noise or generating sidebands at around ±70 Hz on both sides of the peak. For the loop time of 0.384 s, indicated by the open squares and dotted line, the frequency response is worse and the phase shift at 2 Hz is as large as −41 deg; therefore, the field compensation for the 2 Hz ripple is insufficient, though we can expect a full compensation against the major fluctuation component seen in Fig. 2.

Fig. 6 compares the field fluctuation spectrum observed for the 500 MHz NMR magnet and the external sinusoidal field amplitude, which produces a sideband having an amplitude of 5% of the $CHCl_3$ main peak. The horizontal axis shows the sinusoidal frequency and the vertical axis the sinusoidal amplitude. The dashed line at 1.5×10^{-6} (1.5 ppm) is the upper limit of the compensation field of the present spectrometer. If the major fluctuation component seen in Fig. 2 exceeds this critical amplitude, the compensation coil does not work at all, and the spectrometer is unlocked. For the loop time of 0.003 s indicated by the open triangles and red line in Fig. 6, the amplitude curve is two to four orders of magnitude larger than

the field fluctuation spectrum. Therefore, the modulated-sideband in the external current mode is $\ll$5% and is negligible, while, as discussed above, a base line noise at ±70 Hz of the main peak is expected to appear. In contrast, for the loop time of 0.384 s, indicated in this figure by the open squares and the blue line, the amplitude curve is two orders of magnitude lower than the red line, and is close to the field fluctuation spectrum at 2 Hz. Therefore, a noticeable 2 Hz sideband is expected to appear. For the time of 0.083 s, shown by the open circles and green line, the amplitude curve is sufficiently high to avoid a sideband, while no noticeable base line noise appears, and the frequency response peak seen in Fig. 5(a) is negligible. Thus, it is clear that a loop time of 0.08 s is the best choice for NMR measurement in the external current mode.

3.3. Quality of 1D NMR spectra in external current mode

Fig. 7 compares the time dependence of a NMR peak with and without the internal ^{2}H lock in the external current mode. The NMR sample is 1% $CHCl_3$ in acetone-d_6. In the unlocked mode, the NMR peak fluctuates irregularly with a peak–peak amplitude of 170 Hz (0.34 ppm). If we assume a linear change in the field, the modulated FID signal is represented as [26]

$$V_0 \exp\left(-\frac{t}{T_2}\right) \sin\left(2\pi\left(f_0 t + \frac{\mathrm{d}f}{\mathrm{d}t}\frac{t^2}{2}\right)\right), \quad (2)$$

where df/dt corresponds to the rate of change of the field. The Fourier transform of Eq. (2) gives the wiggle in the spectrum; e.g., the third spectrum from the bottom in Fig. 7(a) coincides with the simulated spectrum with df/dt = 2.5 Hz/s, a value close to the actual rate of change of the field seen in Fig. 7(a). Thus, it is clear that the line shape is noticeably modulated, if the spectrometer is operated unlocked in the external current mode.

The effect of the ^{2}H internal lock in the external current mode is shown in Fig. 7(b). The NMR measurement was performed every 2 min over a time period of 28 min. The peak frequency is fixed and the line shape is unchanged. The spectrometer retains the lock mode for about an hour, but then loses the lock, due to the major fluctuation component exceeding the upper limit of the compensation field, ±1.5 ppm.

Fig. 8 shows the ^{1}H lineshape as a function of the feedback loop parameters. The sample is 1% $CHCl_3$ in acetone-d_6, and it rotates at 20 Hz; the sidebands at ±20 Hz are due to sample rotation. The line widths at 50%, 0.55% and 0.11% of the main peak are 0.53 Hz, 8 Hz and 11 Hz, respectively, equivalent to those obtained in the persistent current mode. For the loop time of 0.384 s, seen in Fig. 8(a), the spectrum exhibits a noticeable sideband at ±2 Hz, whose height is 1.5% of that of the main peak. For the loop time of 0.08 s, in Fig. 8(b), the 2 Hz sideband shrinks to less than 0.05% of that of the main peak. For the loop time of 0.003 s in Fig. 8(c), the 2 Hz sideband disappears, while base line noise at ±60–80 Hz is evident. These results agree with the above discussion.

The ^{1}H sensitivity test was conducted for a solution of 0.1% ethyl benzene in $CDCl_3$. The sensitivity, determined by the ratio of the central height of the quartet at 2.7 ppm to the noise over a range of 2 ppm [1], was 578, in good agreement with the sensitivity obtained in the persistent current mode.

The water suppression test was performed with a standard sucrose sample. Water suppression was achieved either by presaturation or by the use of 3919WATERGATE. In the presaturation case, the water signal line widths at 50% and 10% of the DSS peak were 38 Hz and 100 Hz, respectively, close to those obtained in the persistent current mode. The sensitivity, determined by the ratio of the doublet height at 5.4 ppm beside the water signal to the noise over a range of 1.5 ppm, was 111 [27], being close to that obtained in that mode. Thus, the quality of water suppression by presaturation in the external current mode is equivalent to that obtained in the persistent current mode.

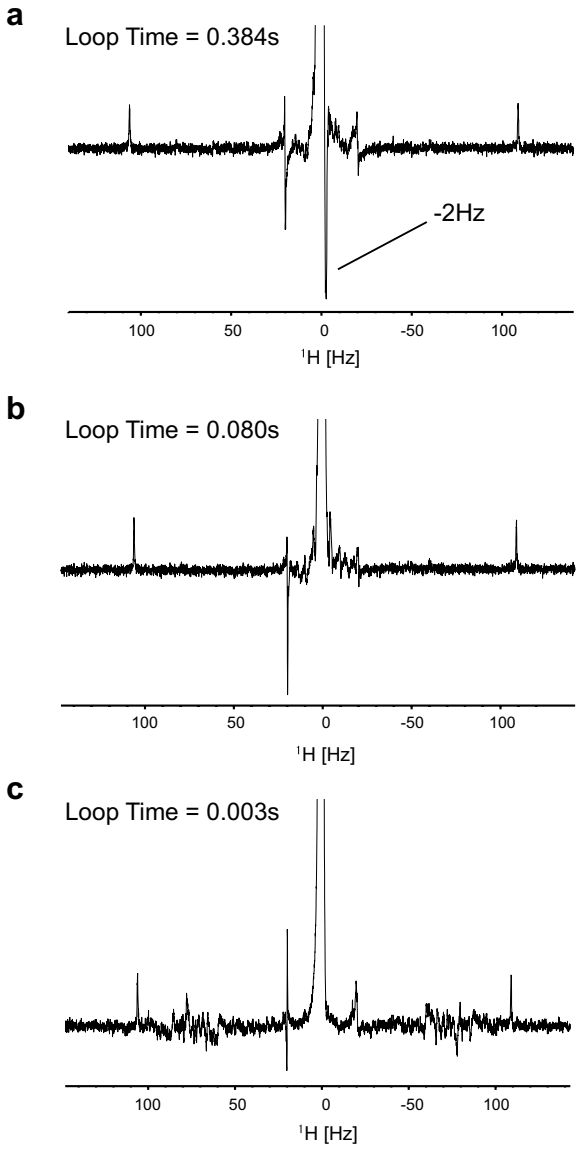

Fig. 8. The lineshape of $CHCl_3$ in acetone-d_6 for loop times of (a) 0.384 s, (b) 0.08 s and (c) 0.003 s. The line shape is very similar to that observed in persistent current mode. For the 0.384 s loop time, a sideband at ±2 Hz is noticeable, while for the 0.003 s loop time, baseline noise at ±60–80 Hz is evident.

In the WATERGATE case, the spectrum was affected by the application of a pulsed field gradient (PFG). If a PFG is used, the ^{2}H internal lock system instantly loses the error signal of the feedback loop. The effect of the PFG depends on the loop time, as the error signal is corrected by the feedback loop on the basis of the recent integral of the error signal over the loop time [27]. Loop times of 0.68 s and 0.08 s are much longer than the field gradient pulse width of ~0.001 s. Therefore, as shown in both Fig. 9(a) and (b), the effect of an instantaneous loss in the error signal is negligible. In contrast, a loop time of 0.003 s is comparable to the gradient field pulse width, and a significant effect is produced when the NMR signal is refocused. Thus, as in Fig. 9(c), the NMR peaks for sucrose disappears.

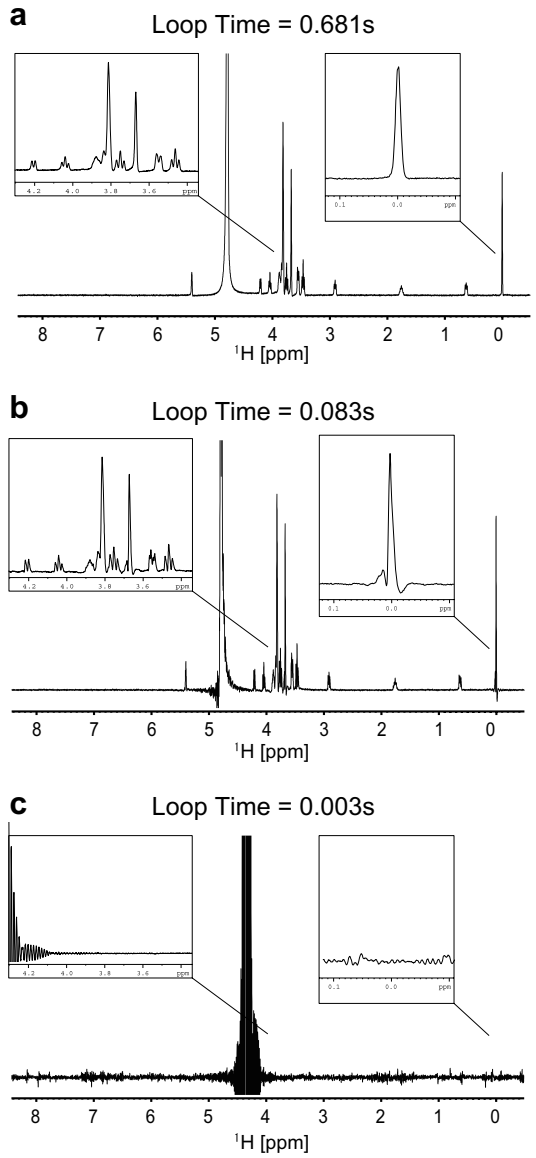

Fig. 9. Water suppression test with 3919WATERGATE for three loop times. The sample is sucrose in 90% H_2O and 10% D_2O: loop times are (a) 0.681 s; (b) 0.083 s and (c) 0.003 s. For the 0.003 s time, a water signal moves to the right and the NMR peaks nearly disappear.

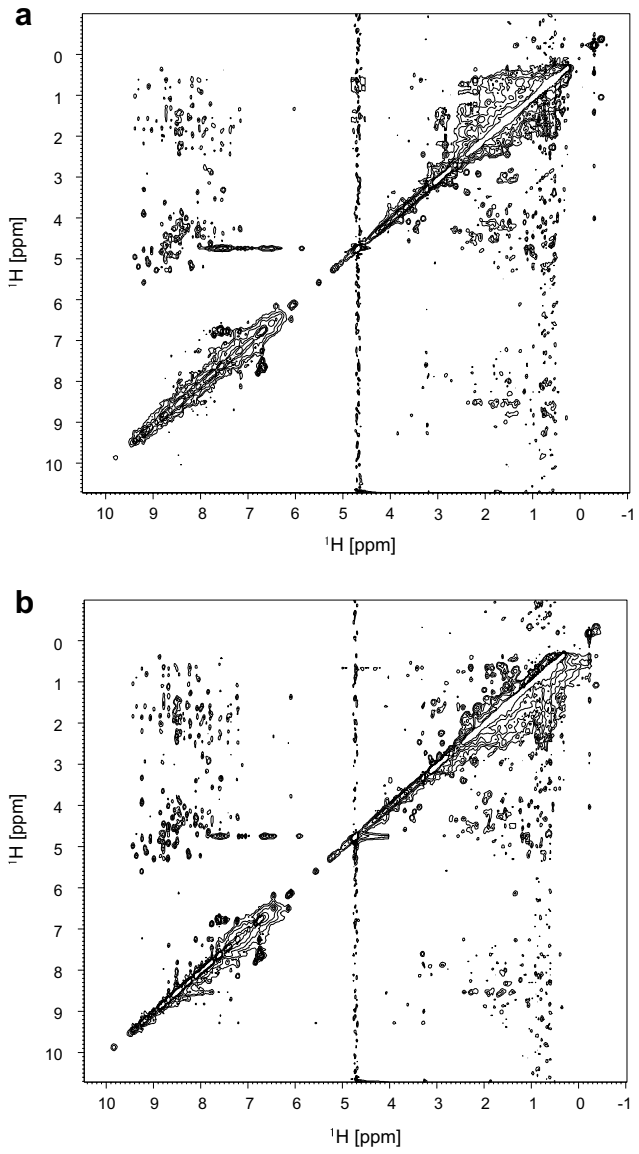

Fig. 10. (a) 3919WATERGATE-NOESY data for chlorella ubiquitin in persistent current mode. (b) 3919WATERGATE-NOESY data observed in external current mode. The loop time is 0.083 s. The quality of the 2D-NOESY data in external current mode is equivalent to that observed in persistent current mode.

3.4. Quality of 2D NMR spectra of chlorella ubiquitin in external current mode

Fig. 10(a) illustrates the 2D-3919WATERGATE NOESY spectrum in persistent current mode, while Fig. 10(b) shows that in external current mode; the same number of peaks is observed in both figures. The optimal loop time of 0.08 s obtained above is used for the NMR measurement. If there is long term instability in the internal ^{2}H lock operation, such as a fluctuation in peak frequency or a change in line shape, noticeable T_1 noise appears along the T_1 axis. Such T_1 noise is not observed in Fig. 10(b) and therefore, we find that the lock is stable over an experimental time interval of 40 min. Furthermore, it is clear that water suppression in external current mode is as good as that in persistent current mode. Similar quality spectra were also obtained for the presaturation-NOESY experiment in external current mode.

Fig. 11(a) illustrates the results of a presaturation-HSQC experiment in persistent current mode, while Fig. 11(b) shows that in external current mode; the loop time is 0.08 s. We identify more than 70 peaks in both spectra, corresponding to the number of residues, 74, of chlorella ubiquitin; no difference is found in chemical shifts, sharpness of the peaks and T_1 noise between the two spectra. Similar results were obtained for the 3919WATERGATE-HSQC in external current mode.

These results demonstrate that the internal ^{2}H lock operates stably over 40 min in external current mode and the quality of 2D NMR spectra are equivalent to those obtained in persistent current mode.

3.5. Further discussion towards beyond-1 GHz solution NMR

Based on the results thus far obtained, we discuss the future viability of a beyond-1 GHz NMR spectrometer and present suggestions of how to overcome remaining problems.

The time interval of the internal ^{2}H lock in external current mode, 40–50 min, is too short for multi-dimensional NMR, where

several tens of hours of data collection are sometimes necessary. The time interval is mainly determined by the major field fluctuation component seen in Fig. 2(a), which occasionally exceeds ±1.5 ppm. Long term stability of the best available DC power supply is ±1 ppm [28]; if we use this DC power supply, we can extend the time interval of the internal ^{2}H lock. However, the upper limit on the compensation field indicated by the broken line in Fig. 6 still limits the time interval of the internal ^{2}H lock. The vendor of the present NMR spectrometer sets the rather low upper limit of ±1.5 ppm on the compensation field; it is sufficient for operation in persistent current mode, but is insufficient for operation in external current mode. If we enhance the upper limit of the compensation field and if we use the best available DC power supply, we may be able to extend the time interval to be sufficient for multi-dimensional NMR measurements. We have started work on such a development.

The current from an external DC power supply is divided into the "open state" (i.e. normal state) superconducting switch R_{open} (∼several Ω) [29], and the NMR coil impedance ωL (L = 200 H); the amount of the ripple current in the NMR coil is proportional to $R_{open}/(R_{open} + j\omega L)$. In case of a beyond-1 GHz NMR magnet, the HTS insert coil is ∼1 H in inductance and generates a static field of about 150 MHz. Therefore, the normalized ripple field amplitude in the 1 GHz NMR magnet (=the ripple field amplitude/1 GHz) is 30-fold larger than that seen in the present experiment. Thus, it is expected that a sideband having several % of the intensity of the main peak appears as a result of these ripples that are often troublesome for high resolution solution NMR. One solution to this problem is to connect the HTS coil in series to Nb_3Sn high-field coils to increase the coil inductance to 100 H; then the normalized ripple fields might decrease to the same level as in the present experiment.

Another problem limiting the time interval of the lock is helium refilling. The NMR magnet uses demountable current leads. When the magnet is operated in external current mode, the power lead is connected to the terminal of the magnet. Heat flow through the current lead results in helium evaporation rate of ∼3 L/h, 100-fold larger than the consumption in persistent current mode; the corresponding helium refill time interval is 10 h. Several of the present authors [19] succeeded in developing a refill-free 600 MHz NMR cryostat, which used both a 4 K-cryocooler to re-liquefy the vaporized helium gas and a thermal-resistive oxide HTS current lead; they succeeded in operating the magnet for over 300 days in external current mode without helium refilling [11,19]. If we use this type of cryostat for a beyond-1 GHz NMR, we will be able to extend the helium refill time interval to more than a year.

In the present experiment, field homogeneity is corrected by initial gradient shimming and then by room temperature shims in persistent current mode. Small field corrections for lower harmonics [30] are sufficient when the magnet operation is changed to the external current mode. On the other hand, in the case of the beyond-1 GHz NMR magnet, we must correct the field homogeneity in external current mode from the beginning of the experiment. To adjust a superconducting shim current, we usually move a small water sphere along the coil axis in a spiral fashion and periodically collect the NMR frequency. They are expanded into Legendre-functions [30], thereby determining the superconducting shim current needed to achieve field homogeneity of 0.1 ppm; to do this we must measure the NMR frequency with an accuracy of ±0.1 ppm, in the presence of field ripple ranging from ±1 to ±10 ppm, which is improbable [21]. Two methods to solve the problem are possible. The first method is to connect a superconducting switch to measure the field distribution in persistent current mode. If a solder joint resistance is 10^{-8} Ω [31] and we have 100 joints in an HTS pancake winding, a persistent current decays 600 ppm in 10 min; the decay is too fast and this method is unlikely to succeed. The second method is to install another external lock with a field stability of ∼0.01 ppm which should allow us to make a field measurement with an accuracy of ±0.1 ppm. Such an external lock is being prepared in RIKEN [32].

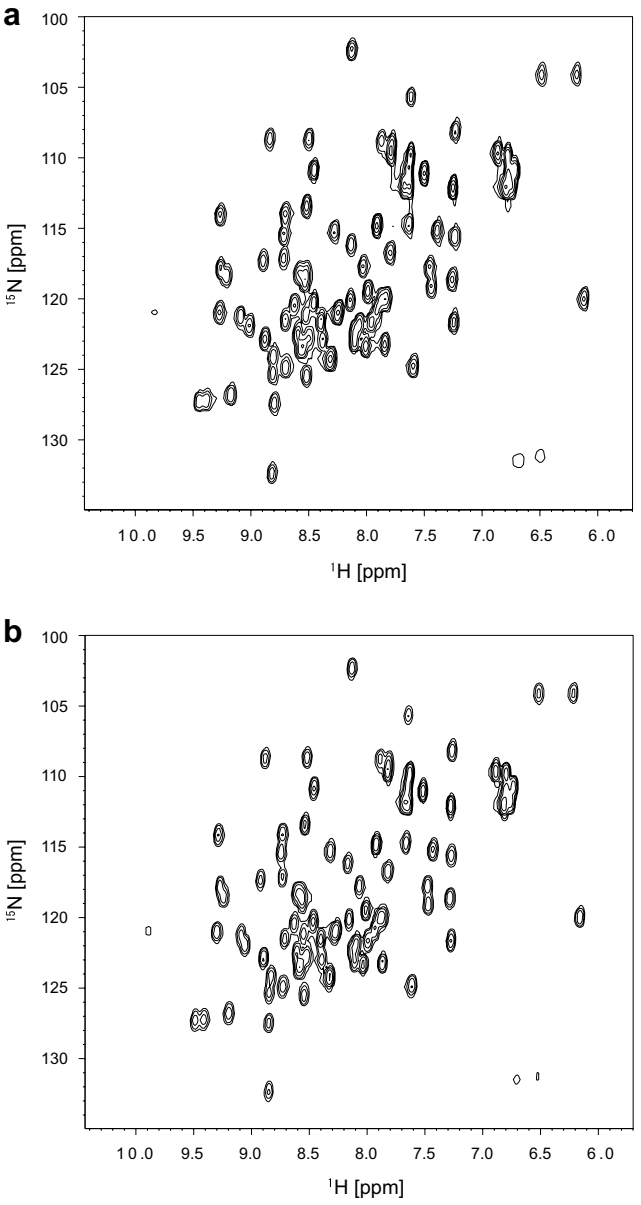

Fig. 11. (a) Presaturation-HSQC data for chlorella ubiquitin in persistent current mode. (b) Presaturation-HSQC data in external current mode. The feedback loop time is 0.083 s. The quality of the 2D-HSQC data in eternal current mode is equivalent to that obtained in persistent mode.

The fast initial change of the field of the NMR magnet operated in persistent current mode is due to decay in the screening current induced during charging of the NMR magnet [33,34]. In the case of a LTS NMR magnet, the screening current is induced in individual LTS filaments. In the case of a HTS magnet, no investigations have been made on the initial change of the magnetic field. Nevertheless, it is reported that a magnetic field remains after discharging the HTS magnet. The phenomenon is interpreted as follows [35,36]; the radial component of the magnetic field penetrates the tape surface, inducing a screening current in the tape conductor. The induced current remains after discharging the HTS magnet, resulting in a residual magnetic field. It is probable that this type of screening current results in a large initial change of the magnetic

field compared with the LTS magnet. We are preparing further experiments in this connection.

4. Conclusions

(1) The field fluctuation by the power supply comprises a major field fluctuation component at low frequencies of 0.003–0.005 Hz and minor field ripples at 2 Hz and 50 Hz. The former limits the time interval of the internal ^{2}H lock, while the latter generates sidebands in NMR spectra measured in the lock mode. Sideband and baseline noise can be controlled by appropriate selection of the feedback loop parameters.
(2) The quality of the 1D NMR spectra obtained in external current mode is equivalent to those obtained in persistent current mode. If the loop time of the feedback loop is as short as PFG width, refocusing is lost resulting in the loss of water suppression and the disappearance of NMR peaks.
(3) The qualities of 2D-NOESY and 2D-HSQC spectra obtained in external current mode are equivalent to those obtained in persistent current mode either with presaturation or 3919WATERGATE. The deuterium lock operates stably over 40–50 min in external current mode, resulting in excellent water suppression and negligible T_1 noise.
(4) To realize a beyond-1 GHz NMR spectrometer, further investigation must be made on (i) the long term stability of a DC power supply, (ii) the enhancement of the compensation field limit for the internal ^{2}H lock, (iii) the extension of the helium refill time interval, and (iv) a method to correct field homogeneity in external current mode.

Acknowledgments

This work is supported by SENTAN, JST in Japan. The authors would like to give their thanks to Mr. Akihiko Yamamoto of Bruker Biospin for his helpful discussions.

References

[1] Andrew E. Derome, Modern NMR Techniques for Chemistry Research, Pergamon Press, Oxford, U.K., 1987.
[2] T. Kiyoshi, H. Maeda, J. Kikuchi, Y. Ito, H. Hirota, S. Yokoyama, S. Ito, T. Miki, M. Hamada, O. Ozaki, S. Hayashi, N. Kurihara, H. Suematsu, M. Yoshikawa, S. Matsumoto, A. Sato, H. Wada, Present status of 920 MHz high resolution NMR spectroscopy, IEEE Trans. Appl. Supercond. 14 (2004) 1608–1612.
[3] K. Pervushin, R. Riek, G. Wider, K. Wüthrich, Attenuated T_2 relaxation by mutual cancellation of dipole–dipole coupling and chemical shift anisotropy indicates an avenue to structures of very large biological macromolecules in solution, Proc. Natl. Acad. Sci. USA 94 (1997) 12366–12371.
[4] R. Riek, G. Wider, K. Pervushin, K. Wüthrich, Polarization transfer by cross-correlated relaxation in solution NMR with very large molecules, Proc. Natl. Acad. Sci. USA 96 (1999) 4918–4923.
[5] Z. Gan, P. Gor'kov, T.A. Cross, A. Samson, D. Massiot, Seeking higher resolution and sensitivity for NMR of quadrupolar nuclei at ultra high magnetic fields, J. Am. Chem. Soc. 124 (2002) 5634–5635.
[6] K. Yamada, S. Dong, G. Wu, Solid-state ^{17}O NMR investigation of the carbonyl oxygen electric-field-gradient tensor and chemical shielding tensor in amides, J. Am. Chem. Soc. 122 (2000) 11602–11609.
[7] http://www.oxinst.com/wps/wcm/connect/Oxford+Instruments/Companies/Oxford+Instruments+Superconductivity+Magnets+Technology/.
[8] T. Hase, Y. Murakami, S. Hayashi, Y. Kawata, Y. Kawate, Bronze route conductors for 1 GHz NMR superconducting magnet, IEEE Trans. Appl. Supercond. 10 (2000) 965–970.
[9] S. Hong, M.B. Field, J.A. Parcell, Y. Zhang, Latest improvement of current carrying capability of niobium tin and its magnet applications, IEEE Trans. Appl. Supercond. 16 (2006) 1146–1151.
[10] N. Ayai, S. Kobayashi, K. Yamazaki, S. Yamada, M. Kikuchi, E. Ueno, J. Fujikami, T. Kato, K. Hayashi, K. Sato, R. Hata, H. Kitaguchi, H. Kumakura, J. Shimoyama, The current transport properties of a 200 A-class Bi-2223 superconducting wire at various temperature and magnetic fields, IEEE Trans. Appl. Supercond. 17 (2007) 3113–3116.
[11] T. Kiyoshi, A. Otsuka, S. Choi, S. Matsumoto, K. Zaitsu, T. Hase, M. Hamada, M. Hosono, M. Takahashi, T. Yamazaki, H. Maeda, NMR Upgrading Project Towards 1.05 GHz, IEEE Trans. Appl. Supercond., in press.
[12] I.R. Dixon, W.D. Markiewicz, K.W. Pickard, C.A. Swenson, Critical current and n-value of Nb_3Sn conductors for the wide bore 900 MHz NMR magnet, IEEE Trans. Appl. Supercond. 9 (1999) 2513–2516.
[13] J. Bascunan, H. Lee, E.S. Bobrov, Y. Iwasa, A low- and high-temperature superconducting NMR magnet: design and performance results, IEEE Trans. Appl. Supercond. 13 (2003) 1550–1553.
[14] H.J. Schneider-Muntau, Y. Nakagawa, Steady State Resistive and Hybrid Magnets, in: F. Herlach, N. Miura (Eds.), High Magnetic Fields: Science and Technology, vol. 1, World Scientific Publishing, Singapore, 2003, pp. 99–152.
[15] K. Hashi, T. Shimizu, A. Goto, T. iijima, S. Ohki, High-field NMR up to 30 T with a hybrid magnet, Jpn. J. Appl. Phys. 44 (2005) 4194–4199.
[16] P.J.M. van Bentum, J.C. Maan, J.W.M. van Os, A.P.M. Kentgens, Strategies for solid-state NMR in high-field Bitter and hybrid magnets, Chem. Phys. Lett. 376 (2003) 338–345.
[17] E.E. Sigmund, V.F. Mitrovic, E.S. Calder, G.W. Thomas, H.N. Bachman, W.P. Halperin, P.L. Kuhns, A.P. Reyes, Inductive shielding of NMR phase noise, J. Mag. Reson. 159 (2002) 190–194.
[18] T. Iijima, K. Takegoshi, K. Hashi, T. Fujito, T. Shimizu, High-resolution NMR with resistive and hybrid magnets: deconvolution using a field-fluctuation signal, J. Mag. Reson. 184 (2007) 258–262.
[19] A. Otsuka, T. Kiyoshi, S. Matsumoto, K. Kominato, M. Takeda, Drift compensation of 600 MHz NMR magnet, IEEE Trans. Appl. Supercond. 17 (2007) 1442–1445.
[20] W. Yao, W. Kim, S. Harn, J. Bascunan, H. Lee, Y. Iwasa, A digital flux injector operated with a 317-MHz NMR magnet, IEEE Trans. Appl. Supercond. 17 (2007) 1450–1453.
[21] J. Bascunan, W. Kim, S. Hahn, E.S. Bobrov, H. Lee, Y. Iwasa, An LTS/HTS magnet operated in the range 600–700 MHz, IEEE Trans. Appl. Supercond. 17 (2007) 1446–1449.
[22] A. Otsuka, T. Kiyoshi, S. Matsumoto, K. Kominato, M. Takada, Field stability of a 600 MHz NMR magnet in the driven-mode operation, IEEE Trans. Appl. Supercond., in press.
[23] K. Wüthrich, NMR studies of structure and function of biological macromolecules (Nobel lecture), Angew. Chem., Int. Ed. 42 (2003) 3340–3363.
[24] F.R. Connor, Modulation, Edward Arnold Ltd., London, 1973.
[25] C. Schmid, Course on dynamics of multidisciplinary and controlled systems. Part III, system control, module version 3.2.2, 2004. Available from: <http://virtual.cvut.cz/dynlabmods/syscontrol.pdf>.
[26] A. Abragam, Principles of Nuclear Magnetism, Oxford Science Publications, Oxford, 1961.
[27] T.D.W. Claridge, High Resolution NMR Techniques in Organic Chemistry, Elsevier, Oxford, 1999.
[28] http://www.danfysik.com/documents/Fact_Sys8500_MPS854_0605_A.pdf.
[29] Y. Iwasa, Case Studies in Superconducting Magnets-Design and Operational Issues, Plenum Press, New York, 1994.
[30] Francoise Romeo, D.I. Hoult, Magnetic field profiling: analysis and correcting coil design, Magnetic Resonance in Medicine 1 (1984) 44–65.
[31] M.N. Wilson, Superconducting Magnets, Clarendon Press, Oxford, 1983.
[32] M. Takahashi, Y. Saito, Y. Yanagisawa, F. Hobo, T. Takao, H. Nakagome, M. Hosono, M. Hamada, T. Kiyoshi, T. Yamazaki, H. Maeda, Towards beyond-1GHz solid state NMR: external lock operation using a frequency counter in external current mode, 49th ENC, W-Th I 139, Asilomar, CA, 2008.
[33] G. Luderer, P. Dullenkopf, Influence of flux penetration on magnetic field stability, Cryogenics (1976) 42–44.
[34] L. Cesnak, J. Kokavec, Magnetic field stability of superconducting magnets, Cryogenics (February) (1977) 107–110.
[35] S. Hahn, J. Bascunan, W.S. Kim, E.S. Bobrov, H. Lee, Y. Iwasa, Presented in the 20th Biennial Conference on Magnet Technology, Manuscript No. 1Q05, 2007.
[36] C. Gu, T. Qu, Z. Han, Measurement and calculation of residual magnetic field in a Bi2223/Ag magnet, IEEE Trans. Appl. Supercond. 17 (2007) 2394–2397.